EXPERIMENTAL STUDY AND FEM-ANALYSIS OF THE MOMENT ON THE BEAM END

SUN Weimin[1] GUO Zhanggen[1] SHEN Dan[1] LUO Yu[1]
[1] College of Civil Engineering, Nanjing University of Technology, China, Email: zhgguo@163.com

ABSTRACT
The problem of the restraint on the beam end from walls for structural masonry buildings with Reinforced Concrete floors has been examined. An experimental study of the restraint on the beam end is described in this paper. The test model is a two-story, one-span masonry structure. The restraint on the beam end, the failure process and failure mode, and the variation in restraining moment and the angle of rotation on the beam were studied. The moment and deflection at the span center were analyzed, and compared with calculated values according to the building code. At the same time, a finite element method (FEM) analysis for evaluating the load deformation process was presented. The restraint due to the nature of the joint, the embedment length of the beam in the wall and the stress on the wall were all studied and were discussed. The effect on the beam restraining moment from increasing the axial stress on the upper wall was obtained. The analytical and experimental results also indicate that a restraining moment exists on the beam end, and that this moment varies with increasing load. The restraining moment on the beam was shown to be affected by the beam stiffness, masonry stiffness, the embedment length of beam in the wall, axial load on the wall, and the nature of the connection of the beam to the wall.

KEYWORDS: composites structure; restraint on the beam end; finite element analysis

INTRODUCTION
Masonry buildings with reinforced concrete (RC) floors offer several advantages including economy and construction, and have been widely used in China. However, in recent years, there have been isolated incidents involving structural masonry buildings with RC floors, which have raised a number of questions about these structures. The problem of the effect on the beam end due to the restriction of the wall in such buildings has been studied[1-3].

For structural masonry buildings with RC floors, the 89 Chinese code for Design of Masonry Structures (GBJ3-88) stipulated that the restraining moment caused by the length of beam embedded in the wall be ignored in the design. Design of Masonry Structures (GBJ50003-2001) stipulates that for multistory buildings with longitudinal load-bearing walls in which the beam span is more than 9 meters, the restraining effect of the wall on the beam end needs to be considered and the moment on the beam end should be calculated considering both ends fixed

for a single span beam. However, when the beam span is smaller than 9 meters, the restraining effect of the wall on the beam end is still not considered.

To verify the difference between the hinged calculation in design and the actual behaviour in structural masonry buildings with RC floors, a two-story, one-span masonry structure was tested, the restriction of the wall on the beam end was studied. The restricting moment was shown to change with the increase in the load. A finite element method (FEM) analysis for evaluating the load deformation process was also carried out. The effect of the inflection of the joint, the length of beam in the wall and stress in the wall on the restriction were all studied. The results of this study are presented here.

DESIGN AND MAKE OF MEMBERS

The model is a two-story, one-span masonry structure. The height of the first story is 1670 mm, and the second story is 1470 mm, with the total height 3140 mm. The depth of wall is 240 mm, the width is 1000 mm. The span of the beam is 3160 mm, and a stiffener is welded in place at the location of loading. The beam end is embedded in a reinforced concrete cushion block which is 240 mm×370 mm×1000 mm and also serves to prevent local compression failure of the top course of masonry. The arrangement and dimensions of the test specimen and experiment are shown in Figures 1 and 2.

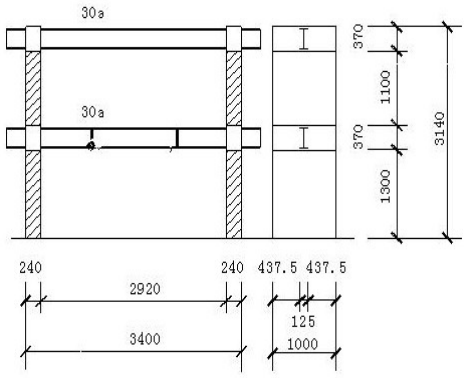

Figure 1: Specimen dimensions

Figure 2: Loading equipment

MATERIAL PROPERTIES

When constructing the specimens, the concrete, KP1 perforated brick,mortar, and resulting masonry were produced according to test standards, maintaining consistency of the components. The mechanical properties of the materials were also determined. The results are shown in Table 1.

Table 1: Average measured compressive strength of experimental materials

material	KP1 perforated brick	mortar	masonry	concrete
Compressive strength（MPa）	9.7	6.94	3.56	32.4

LOADING AND TEST ARRANGEMENT

The test arrangement is shown in Figure 2. The main focus of the experiment was to determine the strain and angle on the beam end, the strain and deflection at the beam mid-span, and the vertical strain on the bottom of wall. A load of 170 kN was first applied at the top of the wall through the jack ,and then a load of 40 kN was applied to the two loading points at the bottom of the steel I-beam to test whether the instrumentation was sensitive and installed reliably. After removing the load, the loading was applied in steps until the structure failed.

FAILURE PROCESS AND FALURE MODE

The behaviour of the specimen can be divided into three stages: 1. Elastic stage: from initial load application to first crack occurring on the outside wall, the specimen behaves elastically. 2. Elastic-plastic stage (crack development). 3. Failure stage: When the load reached 280 kN, the vertical cracks propagate downwards quickly, and the cracks connected with each other by running through the whole wall. At the same time, the inside wall under the steel I-beam crushed and spalled, and the wall reached ultimate state and failed. Refer to Figure 3 for the crack distribution when the wall failed.

Figure 3: Failure mode of specimen

MOMENT ON THE BEAM END

The bending moment on the beam end, the angle of rotation, the mid-span bending moment and the deflection under each level of load in the test are listed in Table 2. For comparison, the theoretical values calculated according to formulae in the code assuming both frame (rigid) and hinged joint conditions.

From the test results, we can see that there is restraining moment on the beam end, which is smaller than that calculated assuming a frame. A seen in Figure 4, the change in moment with load is parabolic in shape and first increases and later decreases. The mid-span bending moment value from the test is always between that calculated according to frame conditions and that calculated assuming hinged joints. The angle of rotation at the beam end and the mid-span deflection are also between the values calculated according to frame and hinge joint conditions. It also reflects that there is restraining moment on the beam end.

Table 2: Comparison of test results and calculated values assuming both rigid joint and hinged joint conditions

	moment on the beam end (kN·m)			angle of rotation on the beam end (rad)		
load(kN)	Test Value M_s	Calculated values according to frame M_k	μ (M_s/M_k)	Test results	Results calculated assuming rigid joints	Results calculated assuming hinged joints
20	5.07	9.28	0.546	0.00032	0.00023	0.00080
40	12.49	18.56	0.673	0.00061	0.00046	0.00162
60	23.80	27.84	0.855	0.00079	0.00070	0.00245
80	26.82	37.11	0.723	0.00098	0.00093	0.00328
100	29.51	46.40	0.636	0.00142	0.00116	0.00412
120	32.17	55.67	0.578	0.00215	0.00139	0.00497
140	34.70	64.96	0.534	0.00250	0.00162	0.00583
160	36.84	74.22	0.469	0.00295	0.00185	0.00669
180	41.45	83.50	0.496	0.00333	0.00209	0.00755
200	40.87	92.78	0.441	0.00378	0.00232	0.00842
210	40.63	97.42	0.417	0.00418	0.00243	0.00886
220	40.46	102.08	0.396	0.00444	0.00255	0.00929
230	40.23	106.70	0.377	0.00500	0.00266	0.00973
240	40.11	111.34	0.36	0.00544	0.00278	0.01017
250	37.68	115.98	0.325	0.00688	0.00290	0.01061
260	37.54	120.62	0.311	0.00783	0.00301	0.01105
270	35.73	125.25	0.285	0.00835	0.00313	0.01149
280	28.40	129.89	0.218	0.00913	0.00324	0.01194

	mid-span bending moment (kN·m)			mid-span deflection (mm)		
load (kN)	Test results	Results calculated assuming rigid joints	Results calculated assuming hinged joints	Test results	Results calculated assuming rigid joints	Results calculated assuming hinged joints
20	6.07	8.08	15.86	0.698	0.647	0.730
40	17.74	16.16	31.94	1.253	1.114	1.481
60	33.59	24.24	48.16	1.832	1.581	2.244
80	43.84	32.32	64.5	2.356	2.048	3.018
100	50.08	40.4	80.93	2.871	2.515	3.801
120	67.97	48.48	97.45	3.226	2.982	4.594
140	82.35	56.55	114.05	3.485	3.449	5.393
160	98.55	64.63	130.73	4.125	3.916	6.200
180	105.28	72.71	147.47	4.853	4.383	7.013
200	125.65	80.79	164.29	5.630	4.850	7.832
210	131.52	84.83	172.71	6.120	5.083	8.244
220	140.28	88.88	181.16	6.508	5.317	8.658
230	148.81	92.91	189.62	7.078	5.550	9.073
240	157.59	96.95	198.09	7.685	5.784	9.489
250	168.49	100.99	206.58	8.078	6.017	9.907
260	175.27	105.03	215.08	8.473	6.251	10.326
270	185.68	109.07	223.6	8.837	6.484	10.747
280	196.57	113.11	232.13	9.935	6.718	11.168

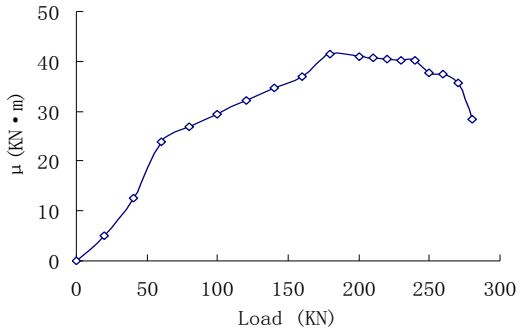

Figure 4: Variation in restricting moment with load

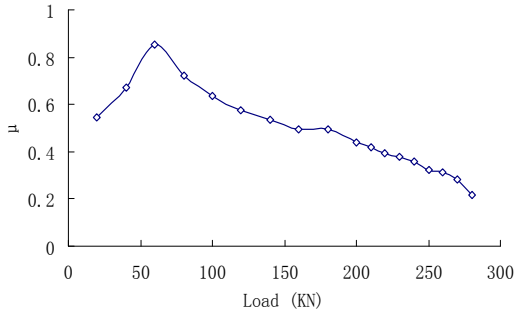

Figure 5: Variation in constraint factor with load

Thee ratio between the restraining moments obtained from the test, M_s, and that calculated assuming frame conditions, M_k, is the constraint factor, μ. μ reflects the degree of comformity between the structure and the frame assumption. The values calculated shown in Table 2 and in Figure 5 for increasing load. From the Figure, we can see that the maximum bending moment on the beam end is 85% of that calculated assuming frame conditions, and the restriction on the beam end from the wall is evident, which reflects the effect of the frame. The value of the restraint factor generally decreases with an increase in the load on the beam, though there is an initial increase in the restriction on the beam end. This is because the rigidity of the restraint degenerates due to the cracks in the walls as the load on the beam increases, and deformation under partial pressure also increases. However, when the masonry is damaged by partial pressure, the restraint still exists. The reason is that when the test piece is damaged, there is no crack at the junction between the upper wall and the steel I-beam, and they are well connected without any separation. So the wall still restricts the beam end to a certain extent.

Table 3 lists the strains measured in the test at the bottom wall, from which we can see that the outside of the bottom wall is always compressed. On the whole, the compression stress increases along with the load on the beam. The inside of the bottom wall is in compression at first but then is subject to tension. It goes back into compression when the wall is near failure. This indicates that the stress distribution at the bottom of the wall is not the same as that of an axially compressed member. It is affected by the axial compression strain and the bending stresses from the beam-wall interaction. Due to the bending induced at the bottom of the wall, the outside of the wall is in compression and the inside is in tension. The moment at the bottom of the wall increases at first, and then decreases.

Table 3: Data of displacement sensor on bottom of wall

load(kN)	20	60	100	140	180	220	240	260	280
Outside the wall($\mu\varepsilon$)	−6	−10	−12	−16	−22	−20	−20	−29	−41
Inside the wall($\mu\varepsilon$)	−1	−2	−3	2	8	5	4	3	−4

FINITE ELEMENT ANALYSIS

The finite element software ANSYS was adopted to perform the nonlinear analysis of the test specimen. On this basis, parameters within the model were varied to analyze the effect of the embedment length of the beam into the wall and the wall stress on the restraining moment on the beam end. Also the calculation methods for the longitudinal bearing wall of multi-story composite structure buildings are investigated and discussed.

ELEMENT TYPE AND MODEL DETAILS

The specimen and load are symmetrical, so only 1/4 of the specimen is modelled. The element Solid concrete 65 is adopted for the building blocks and mortar. Without considering the nonlinearity of the steel I-beam and the cast-in-place concrete cushion block, the element Solid 45 was adopted for the steel I-beam and the cast-in-place concrete cushion block. The model meshing is shown in Figure 6.

The finite element model is divided into two layers. The upper layer is 2.8 m in height with clear span of 6 m. The bottom layer is 2.8 m high. The cross-section dimensions of the reinforced concrete beam are 300 mm x 600 mm. Refer to Figure 7 for the model dimensions and loading

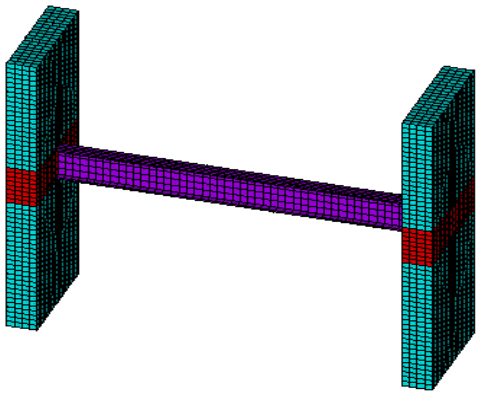

Figure 6: Mesh of the model

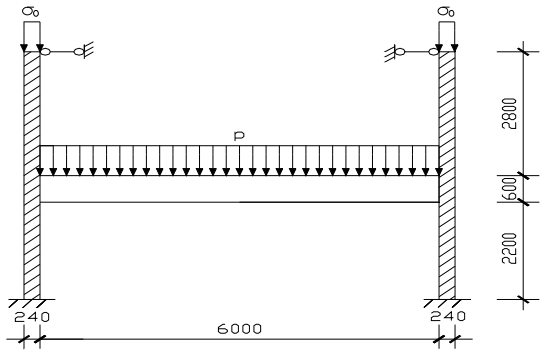

Figure 7: Loading of finite element model

CONSTITUTIVE RELATIONSHIP OF MATERIALS

Research results[8] from Tongji University were adopted for the stress-strain relation in one dimensional stress condition for masonry.

When $\varepsilon \le \varepsilon_0$:

$$\sigma / f_m = \frac{\varepsilon / \varepsilon_0}{0.2 + 0.8\varepsilon / \varepsilon_0} \quad (1)$$

When $\varepsilon > \varepsilon_0$

$$\sigma / f_m = 1.2 - 0.2\varepsilon / \varepsilon_0 \quad (2)$$

Where: $\varepsilon_0 = 0.002$. f_m is the mean value of compressive strength of masonry.

The test value of $\sigma = 3.56MPa$ (0.5162 ksi) is adopted as the value for the compressive strength of the masonry. The initial elastic modulus is 5234 MPa(758.93 ksi). The Poisson ratio is 0.15. In the study of the stress-strain relation of brick masonry in tension, when the tensile stress is not beyond the ultimate tensile strength of masonry, it is considered as elastic, and the value of the initial elastic modulus is adopted in calculations. When the tension stress exceeds the ultimate

tensile strength of masonry, the masonry cracks and does not resist load, therefore the elastic modulus is taken as 0 and the uniaxial tensile strength is adopted as 0.37 MPa(0.05365 ksi).

The elastic modulus of the concrete cushion block is 3.24 MPa(0.4698 ksi) and the Poisson ratio is 0.2. The elastic modulus of the steel I-beam is 2.1×10^5 MPa(0.3045×10^5 ksi), and the Poisson ratio is 0.3.

COMPARISION BETWEEN FE ANALYSIS RESULTS AND TEST RESULTS

The ultimate structural load obtained from finite element calculation is 253.5 kN, which is 90.5% of the test failure load (280 kN). The restraining moment values on the beam end obtained through finite element analysis and the actual test values are compared in Figure 8, from which we can see they are in fair agreement on the whole. It proves the feasibility of finite element analysis method. The reason why the restraining moment values obtained from the finite element analysis are a little greater than the test values is that the nonlinearity of the concrete cushion block is not taken into consideration. As the load on the beam increases, the rigidity of the steel I-beam and concrete cushion block become smaller than the actual rigidities. From the finite element analysis result we can see that there is restraining moment on the beam end, which first increases and then decreases along with the increase of the load on the beam. The curve of the restraining moment is generally parabolic in shape.

The deformation of the model is shown in Figure 9, from which we can see the outside of the top part of the 1st story wall is in tension and the inside is in compression, while the outside of the bottom part of the wall at the ground level is in compression and the inside is in tension. This indicates that there are inflection points in the 1st story wall. The effect of the framework is displayed.

ANALYSIS OF THE RESTRAINING MOMENT ON THE BEAM END

The comparison of results obtained from the finite element analysis and the test, show that the finite element model is reasonable and reliable in predicting the restriction of the wall on the beam end. Therefore, the paramaters of the finite element model were varied in order to analyze the effect of the wall strain, the embedment length of the main beam into the wall, and other factors effecting the restraining moment on the beam end.

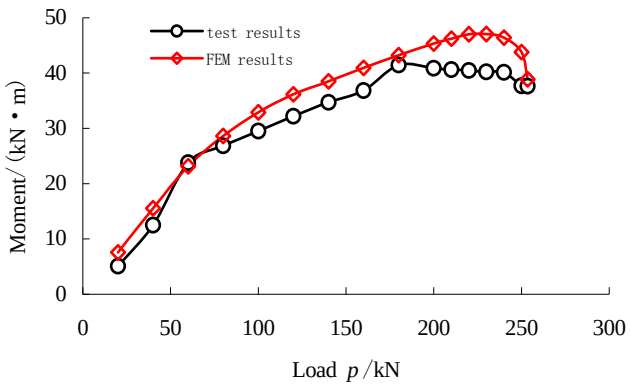

Figure 8: Comparison between test result and FEM analysis result

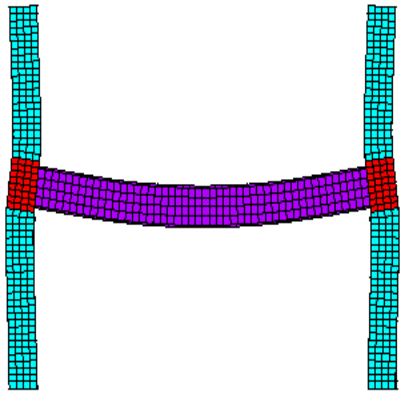

Figure 9: Deformation of finite element model

The behaviour of the longitudinal bearing wall of structural masonry buildings with RC floors mainly depends on the structure of the nodes between the horizontal floor members and walls and their rigidity. According to the ways usually used in engineering at present, 2 types of finite element models were analysed: 1. No beam pad between the beam and the wall. 2. Cast-in-place cushion block with the same width as that of the wall between windows and the same height as that of the beam adopted at the junction between the beam and the wall.

EFFECT OF WALL STRESS

Five load cases were adopted in the finite element analysis: 0 , $0.1 f_m$, $0.2 f_m$, $0.3 f_m$, $0.4 f_m$. Figure 10 shows the variation in restraining moment for different wall stress along for both model type 1 and type 2. The thickness of the wall between windows of the finite element model is 240 mm. The length of the beam inserted in the wall is 240 mm. Examining Figure 10, we observe that as the load on the beam increases, the restraining moment on the beam end first increases and then decreases. The curve is parabolic in shape.

From Figure 10 we can also see that the restraining moment for type 2 is greater than that of type 1, which indicates that the restraining moment of type 2 (at the junction of the beam and the wall a cast-in-place cushion block with the same width as the wall is adopted) is stronger than that of type 1 (no beam pad at the junction of the beam and the wall.).

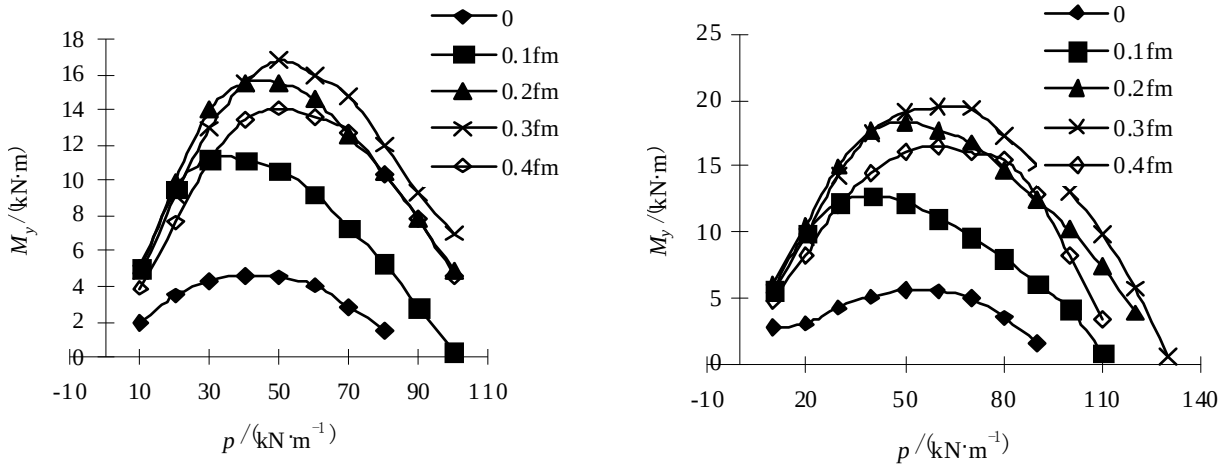

Figure 10: Variation in restraining moment, M_y on the beam for Type 1 model (left) and Type 2 model (right)

EFFECT OF EMBEDMENT LENGTH OF BEAM END

Figure 11 shows the variation in the constraint factor for the beam end with different embedment length. The thickness of the wall between windows in the model is 490 mm. The values of embedment length of the beam ends were 240 mm, 370 mm and 490 mm respectively. The wall stress was $0.2 f_m$. From Figure 11 we observe that the longer the embedment length of the beam into the wall, the larger the restraining moment is.

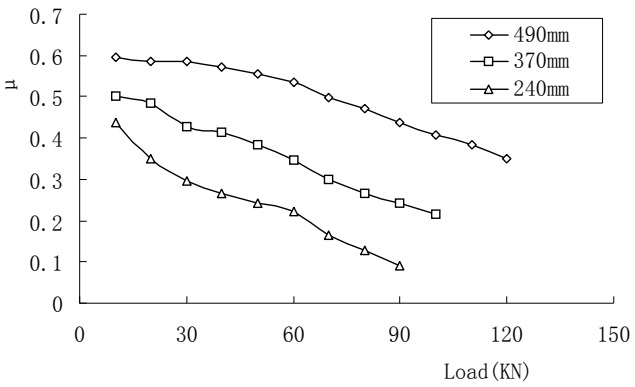

Figure 11: Variation in constraint factor with load

DISCUSSION OF DESIGN CALCULATION METHODS

To discuss the reliability of the calculation methods in the design code, the moment on the beam end of the test specimen is calculated according to the formula from the code for spans more than 9 meters. The comparison of the test results and the calculations is shown in table 4, from which we can see that at the beginning there is a great difference between the calculations and the test results, while at the later stage, especially at the ultimate state, the result of the calculation is basically the same as the test result. This is because the restraining effect on the beam end decreases after the specimen enters the elastic-plastic stage, while the code formula still calculates the result according to the elastic state.

Table 4: Comparison of test results with calculations

load(kN)		20	60	100	140	180	220	240	260	270	280
moment on the beam end （kN.M）	test result	5.07	23.80	29.51	34.70	41.45	40.46	40.11	37.54	35.73	28.40
	calculated value	2.6	7.8	13	18.2	23.4	28.6	31.2	33.8	35.1	36.4
Test result/calculated value		1.95	2.40	2.27	1.91	1.77	1.41	1.29	1.11	1.02	0.78

Both the test results and the finite element analysis show that for multi-story buildings with small span (less than 9 meters), when the beam-slab has a relatively large embedment length into the wall, the wall will generate great restraining effect on the beam ends. Therefore, in the specification, it is regarded that no potential safety hazard will result from the restraining moment on the beam end in multi-story buildings with span less than 9 meters. For structures with cast-in-place cushion block (same width as the wall between windows) at the beam end or flexible sleeper beam fully covering the wall between windows, there is significant restraint on the beam end, and both the wall and the beam may work as that in a rigid frame. It is in this case, unsafe to perform calculations and design according to the hinged joint condition. The restraining moment at the ends of the beam-slab must be considered.

CONCLUSION

The following conclusions are made from the experimental study and nonlinear finite element analysis of the restraining moment that the wall generates on the beam end.

(1) A restraining moment at the ends of beams in structural masonry buildings with RC floors exists. When the vertical load on the wall remains unchanged, the restraining moment on the beam end will follow a parabolic variation characterised by an initial increase and then a decrease as the distributed load on the beam increases. The maximum restraining moment on the beam end reaches 85% of the moment on the beam end calculated assuming rigid frame behaviour. The wall obviously restrains the beam ends, which reflects the effect of the frame.

(2) When the compressive stress on the wall is $\sigma_0 = 0.2 f_m$ or $0.3 f_m$, the restraining moment on the beam end is relatively large. When the compressive stress on the wall is $\sigma_0 = 0.1 f_m$ or $0.4 f_m$, the restraining moment on the beam end is relatively small.

(3) The restraining moment on the beam end increases with an increase of the beam embedment length in the wall.

REFERENCES

1. Chen Zhaoyuan and Kan Yongkui, Building-in effect to beam and slab in multistory composite structure, *Journal of Building Structure* [J]. 1986(2): 28~39
2. Tang Daixin, Wang Guangcai, Zhang Jingji and Sun Weimin, Unloading and restriction effect of masonry at beam ends, *Journal of Building Structure* [J]. 1986 (2): 40~48
3. Sun Weimin, Eccentricity of partial load at beam ends of brick masonry, *Journal of Building Structure* 1994 (1):
4. Tang Daixin and Wang Fenglai, Discussion of calculation diagram of composite structure buildings. *Journal of Harbin University of Civil Engineering and Architecture* [J]. 2000 (10): 15~19
5. Luo Yu, Research of calculation modes of longitudinal bearing wall of multistory composite structure buildings [D]. *Master thesis of Nanjing University of Technology*, May, 2005.
6. Lu Xinzheng and Jiang jianjing, Analyzing complex stress of concrete combined member by ANSYS Solid65 element, *Journal of Harbin University of Civil Engineering and Architecture* [J]. 2003 (6): 22~24.
7. Lu Xilin, Jin Guofang and Wuxiaohan, Theory and application of reinforced concrete nonlinear finite element. Shanghai: T*ongji University Press*, 1997.
8. Zhu Bolong, Design principle of masonry structure, Shanghai: *Tongji University Press*, 1991.
9. Liu Guiqiu, Shi Chuxian and Liu Yibiao, Stress-strain relation of stressed masonry [A], Collection of Thesis in 2000 Masonry Structure Academic Conference, Beijing, China Architecture & Building Press, 2000: 12-18.
10. National Standards of the People's Republic of China, Code for design of masonry structure, Beijing, China Architecture & Building Press, 2001.